

Article

Analyzing Power Beacon Assisted Transmission with Imperfect CSI in Wireless Powered Sensor Networks

Xuanxuan Tang , Wendong Yang *, Yueming Cai and Weiwei Yang

College of Communications Engineering, Army Engineering University of PLA, No. 88 Houbiaoying, Qinhuai District, Nanjing 210007, China; tang_xx@126.com (X.T.); caiym@vip.sina.com (Y.C.); wwyang1981@163.com (W.Y.)

* Correspondence: ywd1110@163.com; Tel.: +86-025-8082-9339

Received: 6 December 2018; Accepted: 18 February 2019; Published: 20 February 2019



Abstract: This paper proposes the maximal ratio transmission (MRT) and maximal ratio combining (MRC) protocols for the power beacon (PB) assisted wireless powered sensor networks and analyzes the impact of the imperfect channel state information (CSI) on the performance using the Markov chain theory. The wireless powered sensor chooses to transmit information to the destination or harvest energy from the PB when its energy can or cannot supply a transmission, respectively. The energy arrival and departure of the sensor is characterized, and the analytical expressions of the network transmit probability, and effective and overall ergodic capacities are formulated and derived. We also optimize the sensor transmit power to maximize the overall ergodic capacity. Our results reveal that the transmit probability and the effective ergodic capacity can be greatly improved with increasing the number of antennas at the PB and the destination, and can also be significantly degraded by decreasing the channel correlation factors. We also demonstrate the effectiveness of the sensor transmit power optimization in improving the overall ergodic capacity.

Keywords: energy harvesting; wireless sensor network; energy storage; power optimization; ergodic capacity

1. Introduction

Energy harvesting (EH) is envisioned to be a promising approach for prolonging the lifetime of energy-constrained networks, typically the wireless sensor networks (WSNs) [1,2]. Traditionally, the energy is harvested from natural sources, e.g., solar, wind, heat, etc. [3]. However, this energy harvesting approach relies on some uncontrollable factors such as weather conditions, thus is not suitable to wireless communication networks that require high stability in terms of the quality-of-service (QoS). Hence, to harvest energy from the radio-frequency (RF) signals, which is capable of providing controllable energy supplies, has gained ever-increasing attention among the wireless communities [4]. An important application scenario of this method lies in wireless power transmission (WPT), which is enabled by the radio-frequency (RF) and is capable of providing convenient and continuous power supply for wireless powered devices [5]. Specifically, classic *time-switching* and *power-splitting* receiving architectures to realize practical WPT are proposed and discussed extensively in the literature [6–8]. To the state of the art, WPT technique has been investigated in numerous systems, e.g., cognitive radio networks [9], multiple-input–multiple-output (MIMO) networks [10], non-orthogonal multiple access (NOMA) networks [11], etc.

While the above works all assume the perfect channel state information (CSI), some recent studies have focused on the effect of imperfect CSI on the system's energy and information transmission. In [12], the secrecy performance of a multiple-input–single-output (MISO) WPT system is studied, where the CSI used for transmit antenna selection (TAS) is outdated. In [13], the power optimization to

maximize the total capacity of small cell in wireless powered heterogeneous networks is investigated, where the imperfect CSI is handled by using a non-cooperative game approach. Meanwhile, Bi and Chen et al. [14] and Liu et al. [15] introduced the Markov chain theory to formulate the dynamic behaviors of energy storage at the wireless powered devices without taking into account the imperfect CSI.

In this paper, we analyze the impact of imperfect CSI on the energy and information transmissions in the wireless powered sensor networks using the Markov chain theory. The PB supplies energy to the wireless powered sensor using MRT protocol if the energy of the sensor is not enough to conduct the transmission operation. Otherwise, the sensor transmits information and the destination receives it using MRC protocol. The differences between this work and the work in [16] are obvious. First, Tang et al. [16] considered the transmission between multiple users and a single-antenna destination, while this work studies the transmission between a single user and a multi-antenna destination. Tang et al. [16] adopted the user selection, while this work does not. Besides, this work adopts MRC at the multi-antenna destination while Tang et al. [16] did not. Moreover, this work considers the effect of imperfect CSI, while Tang et al. [16] only assumed that all the channels were perfect, which becomes a highlight of this work and makes this work much more practical.

The contributions of this paper are summarized as follows:

- To the state of the art, the proposed MRT/MRC WPT system with imperfect CSI is firstly investigated in this paper.
- The network transmit probability, and effective and overall ergodic capacities are derived under the condition of imperfect CSI during both MRT and MRC operations to assess the impact of imperfect CSI on the energy and information transmissions.
- Our results demonstrate the detrimental effect of imperfect CSI on the network transmit probability, effective and overall ergodic capacities, and the validity to improve the overall ergodic capacity by optimizing the sensor transmit power.

2. System Model

We consider a wireless powered sensor network, as shown in Figure 1, which consists of a PB node B , a wireless powered sensor S , and a destination node D . It is assumed that B and D are equipped with N_B and N_D antennas, and S is equipped with a single antenna. The sensor S is equipped with an energy storage with a finite-capacity of ε_T . We assume that all the channels experience quasi-static Rayleigh fading so that the channel coefficients keep constant during a block time T_0 but change independently from one packet time to another [7,17]. Moreover, a standard path-loss model [7] is adopted, namely the average channel power gain $\bar{\gamma}_{ab} = \mathbb{E}[|h_{ab}|^2] = d_{ab}^{-\alpha}$, where $\mathbb{E}[\cdot]$ denotes the expectation operation, α is the path-loss factor, and h_{ab} and d_{ab} denote the channel coefficient and the distance between a and b , respectively.

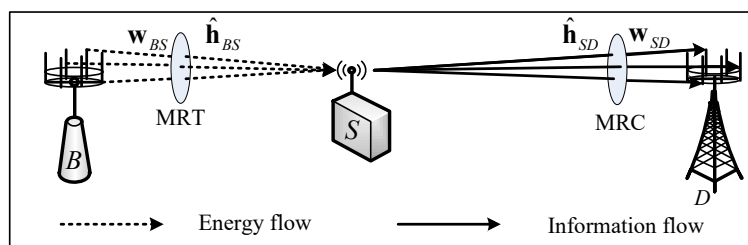


Figure 1. System model.

To quantify the energy storage at the sensor, we adopt a discrete-level model similar to in [14,15]. Specifically, the energy capacity of the storage is discretized into L units. As such, there will be $1 + L$ possible energy levels in total at S with the l th energy level defined as

$$\varepsilon_l = l \cdot \varepsilon_\Delta, \quad l \in \{0, 1, \dots, L\}, \quad (1)$$

where $\varepsilon_\Delta = \frac{\varepsilon_T}{L}$ is the single energy unit.

Obviously, an energy amount $P_S T_0$ is required to supply a transmission operation (note that the extra power consumption of the transmitting/receiving circuitry is neglected in this paper [7,8]), where P_S represents the sensor transmit power. We set $P_S = l_S \frac{\varepsilon_\Delta}{T_0}$ in this paper due to the energy discretization [14], where l_S denotes the transmit energy level corresponding to the energy consumed at S of each transmission with $l_S \in \{1, \dots, L\}$. We highlight that the sensor energy will always transfer within $\{\varepsilon_l\}_{l=0}^L$ given in Equation (1), and the transitions among energy levels form a Markov chain [14]. For the notation convenience, we denote the stationary probability vector of the Markov chain as $\boldsymbol{\pi} = [\pi_0, \pi_1, \dots, \pi_l, \dots, \pi_L]^T$, where π_l is the stationary probability of the l th energy level ε_l .

2.1. Information Transmitting for $l \geq l_S$

When the index of the energy level at S satisfies $l \geq l_S$, the sensor energy will be sufficient so that information transmission can occur at S . As a result, the received signal-to-noise ratio (SNR) at D could be given by

$$\gamma_D = \gamma_S \left| \mathbf{h}_{SD}^T \mathbf{w}_{SD} \right|^2, \quad (2)$$

where $\gamma_S = \frac{P_S}{N_0}$, and N_0 is the variance of the additive white Gaussian noise (AWGN). $\mathbf{h}_{SD} = [h_{SD_1}, \dots, h_{SD_d}, \dots, h_{SD_{N_D}}]^T \in \mathbb{C}^{N_D \times 1}$ represents the channel coefficient vector between S and D with $d \in \{1, \dots, N_D\}$, \mathbf{w}_{SD} is the normalized MRC weight vector applied at D satisfying $\mathbf{w}_{SD} = \frac{\hat{\mathbf{h}}_{SD}}{\|\hat{\mathbf{h}}_{SD}\|}$ due to imperfect CSI [18], and $\hat{\mathbf{h}}_{SD}$ is the estimated channel coefficient vector of \mathbf{h}_{SD} that can be modeled as [12,19]

$$\hat{\mathbf{h}}_{SD} = \rho_{SD} \mathbf{h}_{SD} + \sqrt{1 - \rho_{SD}^2} \mathbf{e}_{SD}, \quad (3)$$

where ρ_{SD} denotes the channel correlation factor between the actual channel coefficient vector \mathbf{h}_{SD} and its estimation $\hat{\mathbf{h}}_{SD}$, and \mathbf{e}_{SD} is the Gaussian random estimating error vector with each element having the variance of $\tilde{\gamma}_{SD}$.

2.2. Information Transmitting for $l < l_S$

When the index of the energy level at S satisfies $l < l_S$, the energy harvesting will occur, and the harvested energy at S would be

$$\varepsilon_S = \eta T_0 P_B \left| \mathbf{h}_{BS}^T \mathbf{w}_{BS} \right|^2, \quad (4)$$

where P_B is the transmit power of B and η denotes the energy conversion efficiency. \mathbf{h}_{BS} represents the channel coefficient vector between B and S with $b \in \{1, \dots, N_B\}$, $\mathbf{w}_{BS} \in \mathbb{C}^{N_B \times 1}$ is the normalized MRT weight vector applied at B satisfying $\mathbf{w}_{BS} = \frac{\hat{\mathbf{h}}_{BS}}{\|\hat{\mathbf{h}}_{BS}\|}$ due to imperfect CSI, and $\hat{\mathbf{h}}_{BS}$ is the estimated channel coefficient vector of \mathbf{h}_{BS} that can be modeled as [12,19]

$$\hat{\mathbf{h}}_{BS} = \rho_{BS} \mathbf{h}_{BS} + \sqrt{1 - \rho_{BS}^2} \mathbf{e}_{BS}, \quad (5)$$

where ρ_{BS} denotes the channel correlation factor between the actual channel coefficient vector \mathbf{h}_{BS} and its estimation $\hat{\mathbf{h}}_{BS}$, and \mathbf{e}_{BS} is the Gaussian random estimating error vector with each element having the variance of $\bar{\gamma}_{BS}$. Then, the harvested energy that can be saved in the storage of S after energy discretization is derived as [14,15]

$$\tilde{\varepsilon}_S = \varepsilon_{l^*}, \text{ with } l^* = \arg \max_{l \in \{0,1,\dots,L\}} \{\varepsilon_l : \varepsilon_l \leq \varepsilon_S\}. \tag{6}$$

3. Ergodic Capacity

The ergodic capacity is defined as the expected value of the instantaneous mutual information of the received SNR [20]. By using the total probability theorem, the overall ergodic capacity of the proposed network can be calculated as

$$\bar{C} = P_{tp} \bar{C}_{tp}, \tag{7}$$

where $P_{tp} = \sum_{l=1}^L \pi_l$ is the transmit probability of the network, and \bar{C}_{tp} denotes the effective ergodic capacity of the network on condition that the information transmission occurs, which is defined as [19,20]

$$\bar{C}_{tp} = \mathbb{E}[\log_2(1 + \gamma_D)] = \frac{1}{\ln 2} \int_0^\infty \frac{1 - F_{\gamma_D}(x)}{1 + x} dx. \tag{8}$$

Next, we elaborate on the derivation of \bar{C}_{tp} and P_{tp} , and then focus on the optimization of P_S to maximize \bar{C} .

3.1. Derivation of Effective Ergodic Capacity \bar{C}_{tp}

Referring to ([18], Equation (48)), the cumulative distribution function (CDF) of γ_D is given by

$$F_{\gamma_D}(x) = 1 - e^{-\frac{x}{\gamma_S \bar{\gamma}_{SD}}} \sum_{m=0}^{N_D-1} \sum_{k=0}^m \frac{\psi_m}{k!} \left(\frac{x}{\gamma_S \bar{\gamma}_{SD}}\right)^k, \tag{9}$$

where $\psi_m = \frac{(N_D-1)! \rho_{SD}^{2m} (1-\rho_{SD}^2)^{N_D-m-1}}{(N_D-m-1)! m!}$, and $F_\gamma(\cdot)$ represents the CDF of random variable γ . Differentiating Equation (9) in the cases of $k = 0$ and $k > 0$, we have

$$1 - F_{\gamma_D}(x) = e^{-\frac{x}{\gamma_S \bar{\gamma}_{SD}}} \left[\sum_{m=0}^{N_D-1} \psi_m + \sum_{m=1}^{N_D-1} \sum_{k=1}^m \frac{\psi_m}{k!} \left(\frac{x}{\gamma_S \bar{\gamma}_{SD}}\right)^k \right]. \tag{10}$$

Substituting Equation (10) into Equation (8), we derive \bar{C}_{tp} as

$$\bar{C}_{tp} = \frac{1}{\ln 2} \sum_{m=0}^{N_D-1} \psi_m \underbrace{\int_0^\infty \frac{e^{-\frac{x}{\gamma_S \bar{\gamma}_{SD}}}}{1+x} dx}_{\mathcal{I}_1} + \frac{1}{\ln 2} \sum_{m=1}^{N_D-1} \sum_{k=1}^m \frac{\psi_m}{k!} \underbrace{\int_0^\infty \frac{e^{-\frac{x}{\gamma_S \bar{\gamma}_{SD}}}}{1+x} \left(\frac{x}{\gamma_S \bar{\gamma}_{SD}}\right)^k dx}_{\mathcal{I}_2}. \tag{11}$$

Resorting to ([21], eq. (3.352.4)) and ([21], eq. (3.353.5)), we derive \mathcal{I}_1 and \mathcal{I}_2 as

$$\mathcal{I}_1 = -Ei\left(\frac{-1}{\gamma_S \bar{\gamma}_{SD}}\right) e^{\frac{1}{\gamma_S \bar{\gamma}_{SD}}}, \tag{12}$$

$$\mathcal{I}_2 = \sum_{k_0=1}^k (k_0 - 1)! \left(\frac{-1}{\gamma_S \bar{\gamma}_{SD}}\right)^{k-k_0} - \left(\frac{-1}{\gamma_S \bar{\gamma}_{SD}}\right)^k Ei\left(\frac{-1}{\gamma_S \bar{\gamma}_{SD}}\right) e^{\frac{1}{\gamma_S \bar{\gamma}_{SD}}}. \tag{13}$$

Substituting Equations (12) and (13) into Equation (11), we easily derive \bar{C}_{tp} .

3.2. Derivation of Transmit Probability P_{tp}

From the calculation expression of P_{tp} given after Equation (7), we need to derive the stationary probability vector of the Markov chain π . According to the Markov chain theory, to derive π , we need to figure out the transition probabilities among all the energy levels first. Without loss of generality, we examine the transition probability from ε_l to $\varepsilon_{l'}$ within one transition, $l, l' \in \{0, 1, \dots, L\}$.

3.2.1. Transition for $l \geq l_S$

As described in Section 2, the sensor will transmit information when $l \geq l_S$ so that the energy in its storage will decrease ε_{l_S} . As a result, the transition probability from ε_l to $\varepsilon_{l'}$ will be $P_{l,l'} = 1$ only when $\Delta l = -l_S$, where $\Delta l = l' - l$.

3.2.2. Transition for $l < l_S$

For $l < l_S$, the sensor will be not able to transmit information and has to harvest energy from the PB. Therefore, $\Delta l < 0$ is not possible to occur because the energy saved in the storage is not possible to decrease if energy harvesting is occurred. For the case with $\Delta l \geq 0$ and $l' < L$, we know that there would be an energy increment of $\varepsilon_{\Delta l}$ only when the harvested energy ε_S satisfying $\varepsilon_{\Delta l} \leq \varepsilon_S < \varepsilon_{\Delta l+1}$, which results in $P_{l,l'} = F_{\varepsilon_S}(\varepsilon_{\Delta l+1}) - F_{\varepsilon_S}(\varepsilon_{\Delta l})$ with ε_S given in Equation (4). On the contrary, the event of $\Delta l \geq 0$ and $l' = L$ will occur as long as $\varepsilon_S \geq \varepsilon_{\Delta l}$, which leads to $P_{l,l'} = 1 - F_{\varepsilon_S}(\varepsilon_{\Delta l})$.

As such, the transition probability from ε_l to $\varepsilon_{l'}$ within one transition is summarized as

$$P_{l,l'} = \begin{cases} 1, & l \geq l_S, \Delta l = -l_S, \\ F_{\varepsilon_S}(\varepsilon_{\Delta l+1}) - F_{\varepsilon_S}(\varepsilon_{\Delta l}), & l < l_S, \Delta l \geq 0, l' < L, \\ 1 - F_{\varepsilon_S}(\varepsilon_{\Delta l}), & l < l_S, \Delta l \geq 0, l' = L, \\ 0, & \text{others.} \end{cases} \quad (14)$$

We note that the CDF of ε_S in Equation (14) could be readily derived from Equation (9) by making an appropriate replacement, i.e., $\gamma_S \rightarrow \eta T_0 P_B$, $\tilde{\gamma}_{SD} \rightarrow \tilde{\gamma}_{BS}$, $N_D \rightarrow N_B$, $\rho_{SD} \rightarrow \rho_{BS}$. This can be easily concluded because the weight vector of MRC \mathbf{w}_{SD} has the similar form with the weight vector of MRT.

Denote $\mathbf{A} \in \mathbb{R}^{(L+1) \times (L+1)}$ as the transition matrix with its $(l+1, l'+1)$ th element being $\mathbf{A}_{(l+1),(l'+1)} = P_{l,l'}$. It is easy to know that \mathbf{A} is irreducible and row stochastic. Hence, the stationary probability vector can be derived as [14,15]

$$\pi = (\mathbf{A}^T - \mathbf{E} + \mathbf{Q})^{-1} \mathbf{b}, \quad (15)$$

where $\mathbf{b} = (1, 1, \dots, 1)^T$, \mathbf{E} is the identity matrix, and \mathbf{Q} is an all-ones matrix. Hence, $P_{tp} = \sum_{l=l_S}^L \pi_l$ can be then derived.

3.3. Sensor Transmit Power Optimization

From the overall ergodic capacity definition in Equation (7), we see that there exists a trade-off between the value of P_S and the overall ergodic capacity of the network. On the one hand, increasing P_S leads to decreased P_{tp} , and then degrades overall ergodic capacity. On the other hand, increasing P_S also results in increased \bar{C}_{tp} , and thus is beneficial to improve the overall ergodic capacity at the same time. As a result, there exists an optimum sensor transmit power P_S^* to maximize the overall

ergodic capacity of the considered network. Mathematically, the optimization of P_S to maximize the overall ergodic capacity can be modeled as

$$P_S^* = I_S^* \frac{\epsilon \Delta}{T_0} = \frac{\epsilon \Delta}{T_0} \arg \max_{I_S} \bar{C}(I_S), \tag{16}$$

$$s.t. \quad I_S \in \{1, 2, \dots, L\}.$$

Note that the closed-form expression of P_S^* is intractable. As an alternative, it can be solved by applying the exhaustive method conveniently because it is an one-dimensional problem and the argument I_S only takes finite values.

4. Numerical Results

In this section, we present the numerical results to illustrate the impacts of various system parameters on the performance of the proposed network. Without loss of generality, we set $P_B = 40$ dBm, $\epsilon_T = 50$ mJ, $L = 10$, $\eta = 0.8$, $\alpha = 3$, $\rho_{BS} = \rho_{SD} = \frac{2}{3}$, $N_B = N_D = 3$, $d_{BS} = 10$ m, $d_{SD} = 300$ m, $T_0 = 1$ s, and $N_0 = -60$ dBm, unless otherwise stated.

Figures 2 and 3 plot the transmit probability P_{tp} of the proposed network versus the channel correlation factor between B and S , ρ_{BS} , and the sensor transmit power P_S , respectively. We note that $N_B \geq 2$ is required to conduct MRT operation, and the case of $N_B = 1$ is presented as a benchmark when MRT is not applied. As can be expected, the energy transmission is greatly improved due to MRT with N_B increases, so that P_{tp} is largely improved. However, P_{tp} will be significantly degraded with decreasing ρ_{BS} . Specifically, the MRT operation does not bring any benefit when $\rho_{BS} = 0$ regardless of the value of N_B . This is because there is little correlation between \mathbf{h}_{SD} and $\hat{\mathbf{h}}_{SD}$ with $\rho_{BS} = 0$. Besides, we find from the results in Figure 3 that P_{tp} will severely decrease with the increase of P_S . The reason is that a larger transmit power is generally more difficult to be satisfied for the wireless powered sensor.

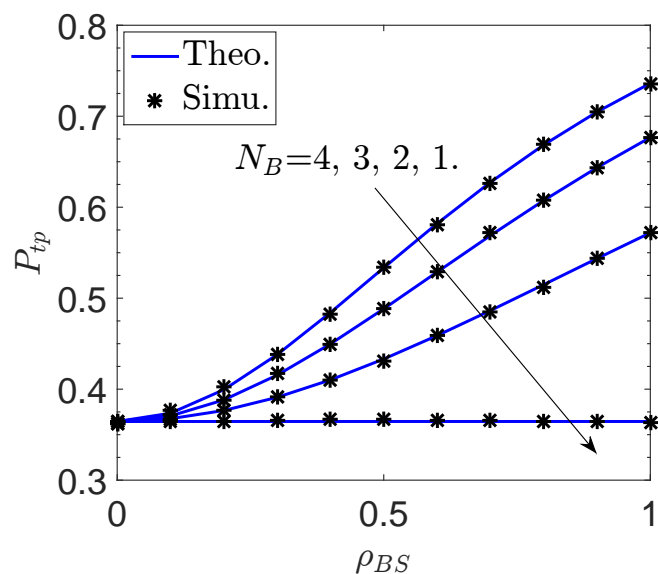


Figure 2. Transmit probability P_{tp} of the proposed network vs. the channel correlation factor ρ_{BS} .

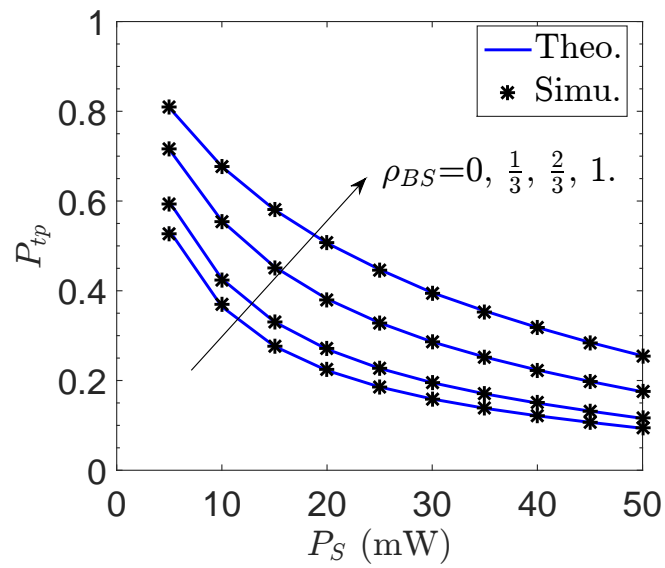


Figure 3. Transmit probability P_{tp} of the proposed network vs. the sensor transmit power P_S .

Figures 4 and 5 plot the effective ergodic capacity \bar{C}_{tp} of the proposed network versus the channel correlation factor between S and D , ρ_{SD} , and the sensor transmit power P_S , respectively. Similarly, the effective ergodic capacity \bar{C}_{tp} can be enhanced by increasing the number of antennas at D , which however degrades with the decrease of ρ_{SD} . Specifically, the MRC becomes invalid when $\rho_{SD} = 0$ regardless of the value of N_D . Moreover, it is observed in Figure 5 that \bar{C}_{tp} can be improved by increasing the sensor transmit power, because a larger sensor transmit power generally leads to a greater received SNR at D .

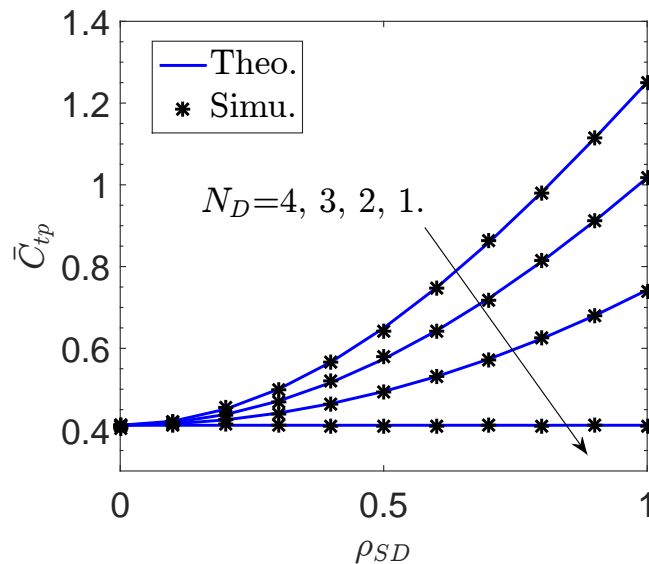


Figure 4. Effective ergodic capacity \bar{C}_{tp} of the proposed network vs. the channel correlation factor ρ_{SD} .

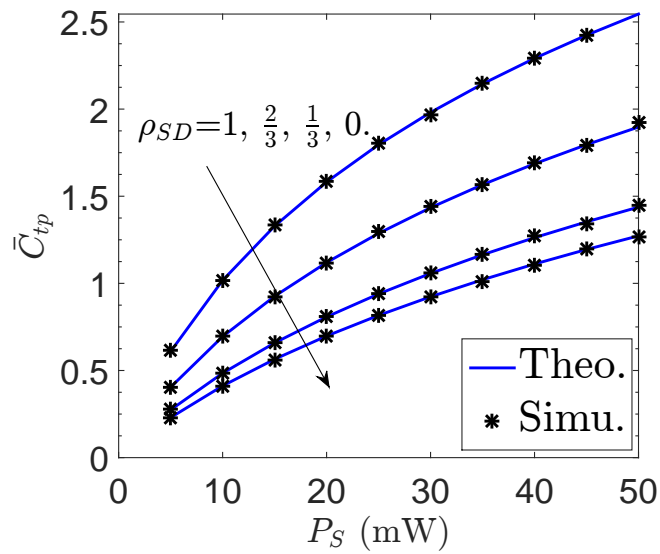


Figure 5. Effective ergodic capacity \bar{C}_{tp} of the proposed network vs. the sensor transmit power P_S .

Figures 6 and 7 plot the overall ergodic capacity \bar{C} of the proposed network versus the sensor transmit power P_S , the number of antennas at B , N_B , and the channel correlation factor between B and S , ρ_{BS} , respectively. In Figure 6, a trade-off between the value of P_S and ergodic capacity is observed for various N_B and ρ_{BS} . In addition, Figure 7 presents the maximized overall ergodic capacity \bar{C} with different sensor transmit power. Note that, in this figure, $l_S = 1$ and $l_S = L$ correspond to $P_S = 5$ mW and $P_S = 50$ mW, respectively. As can be seen, the overall ergodic capacity can be greatly improved with the proposed sensor transmit power optimization.

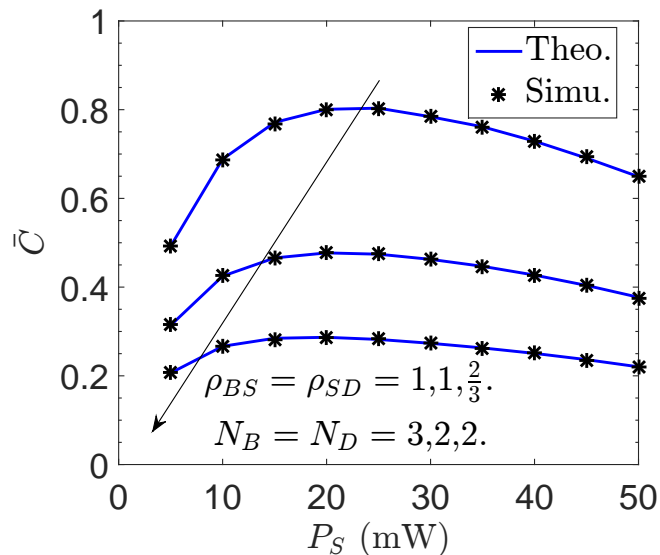


Figure 6. Overall ergodic capacity \bar{C} of the proposed network vs. the sensor transmit power P_S .

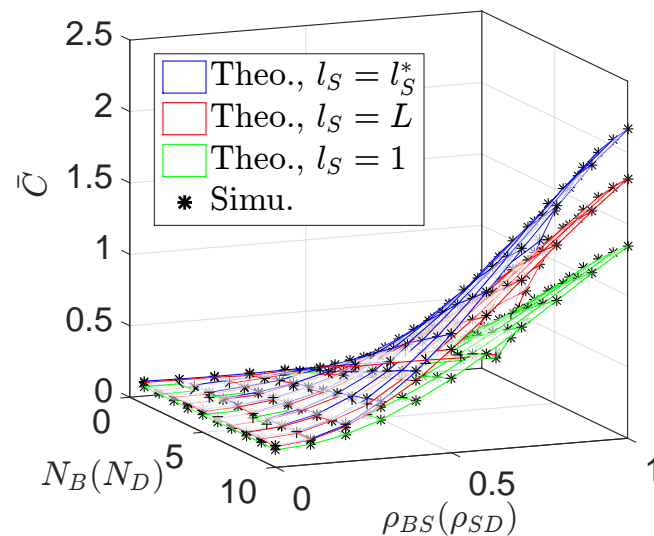


Figure 7. Overall ergodic capacity \bar{C} of the proposed network vs. the number of antennas N_B and the channel correlation factor ρ_{BS} .

5. Application and Future Work

WPT technique can have potential applications in various scenarios of low power devices. Promising applications include health-care monitoring by implantable bio-medical sensors, architectural structure monitoring using embedding sensors in bridges, building, roads, etc. Besides, this technique can also be widely applied in the emerging construction of smart city, where numerous home-based low power wireless devices can be effectively and conveniently powered. For example, in 2017, the PB-based product “Cota Tile” was designed by Ossia Inc. to charge wireless devices at home, which received the “Innovation Awards” at the 2017 Consumer Electronics Show (CES) [22]. However, WPT technique also imposes various challenging issues to be addressed before it becomes a key technology for the future communications systems. For example, hardware development is greatly needed so that the harvesting circuits can obtain as much energy as possible. Besides, communication and energy security must be carefully considered in such systems. Overall, for the successful application of WPT systems, numerous challenges must be tackled at a cross-layer perspective from hardware implementation to specific architectural design.

6. Conclusions

PB assisted information and energy transmissions in the wireless powered sensor networks were studied taking into account the imperfect CSI. The energy arrival and departure of the finite-capacity storage at the sensor were characterized by adopting the Markov chain theory, and the analytical expressions of the network transmit probability, and effective and overall ergodic capacities were formulated and obtained. In addition, the sensor transmit power optimization to maximize the overall ergodic capacity was solved. The results indicate that the network transmit probability and the effective ergodic capacity could be greatly improved by increasing the number of antennas at the PB and the destination, respectively. Moreover, it was depicted that the transmit probability and the effective ergodic capacity would be severely degraded by decreasing the channel correlation factors. The findings also illustrate the validity of optimizing the sensor transmit power to improve the overall ergodic capacity of the proposed network.

Author Contributions: Conceptualization, X.T. and W.Y. (Wendong Yang); Funding acquisition, Y.C.; Investigation, X.T.; Methodology, X.T. and W.Y. (Weiwei Yang); Project administration, Y.C.; Supervision, W.Y. (Wendong Yang)

and Y.C.; Validation, W.Y. (Wendong Yang); Writing—original draft, X.T.; and Writing—review and editing, X.T., W.Y. (Wendong Yang) and W.Y. (Weiwei Yang).

Funding: This work was supported by the National Natural Science Foundation of China under grant No. 61771487.

Acknowledgments: The authors would like to extend their gratitude to the anonymous reviewers for their valuable and constructive comments, which have largely improved and clarified this paper.

Conflicts of Interest: The authors declare no conflict of interest.

Abbreviations

The following abbreviations are used in this manuscript:

| | |
|------|----------------------------------|
| AWGN | Additive white Gaussian noise |
| CDF | Cumulative distribution function |
| CSI | Channel state information |
| EH | Energy harvesting |
| MISO | Multiple-input-single-output |
| MRC | Maximal ratio combining |
| MRT | Maximal ratio transmission |
| PB | Power beacon |
| RF | Radio-frequency |
| TAS | Transmit antenna selection |
| WPT | Wireless power transmission |
| WSN | wireless sensor networks |

References

1. Qian, L.P.; Feng, G.; Leung, V.C.M. Optimal Transmission Policies for Relay Communication Networks with Ambient Energy Harvesting Relays. *IEEE J. Sel. Areas Commun.* **2016**, *34*, 3754–3768. [[CrossRef](#)]
2. Sudevalayam, S.; Kulkarni, P. Energy Harvesting Sensor Nodes: Survey and Implications. *IEEE Commun. Surv. Tutor.* **2011**, *13*, 443–461. [[CrossRef](#)]
3. Nasir, A.A.; Zhou, X.; Durrani, S.; Kennedy, R.A. Relaying protocols for wireless energy harvesting and information processing. *IEEE Trans. Wirel. Commun.* **2013**, *12*, 3622–3636. [[CrossRef](#)]
4. Mohjazi, L.; Dianati, M.; Karagiannidis, G.K.; Muhaidat, S.; Al-Qutayri, M. RF-powered cognitive radio networks: Technical challenges and limitations. *IEEE Commun. Mag.* **2015**, *53*, 94–100. [[CrossRef](#)]
5. Ibrahim, A.M.; Ercetin, O.; ElBatt, T. Stability Analysis of Slotted Aloha With Opportunistic RF Energy Harvesting. *IEEE J. Sel. Areas Commun.* **2016**, *34*, 1477–1490. [[CrossRef](#)]
6. Zhou, X.; Zhang, R.; Ho, C.K. Wireless Information and Power Transfer: Architecture Design and Rate-Energy Tradeoff. *IEEE Trans. Commun.* **2013**, *61*, 4754–4767. [[CrossRef](#)]
7. Zhong, C.; Suraweera, H.A.; Zheng, G.; Krikidis, I.; Zhang, Z. Wireless Information and Power Transfer With Full Duplex Relaying. *IEEE Trans. Commun.* **2014**, *62*, 3447–3461. [[CrossRef](#)]
8. Wang, D.; Zhang, R.; Cheng, X.; Yang, L. Capacity-Enhancing Full-Duplex Relay Networks based on Power Splitting (PS-)SWIPT. *IEEE Trans. Veh. Technol.* **2017**, *66*, 5445–5450. [[CrossRef](#)]
9. Shah, S.T.; Choi, K.W.; Lee, T.J.; Chung, M.Y. Outage Probability and Throughput Analysis of SWIPT Enabled Cognitive Relay Network with Ambient Backscatter. *IEEE Internet Things J.* **2018**, *5*, 3198–3208. [[CrossRef](#)]
10. Wen, Z.; Liu, X.; Beaulieu, N.C.; Wang, R.; Wang, S. Joint Source and Relay Beamforming Design for Full-Duplex MIMO AF Relay SWIPT Systems. *IEEE Commun. Lett.* **2016**, *20*, 320–323. [[CrossRef](#)]
11. Yang, Z.; Ding, Z.; Fan, P.; Al-Dhahir, N. The Impact of Power Allocation on Cooperative Non-orthogonal Multiple Access Networks With SWIPT. *IEEE Trans. Wirel. Commun.* **2017**, *16*, 4332–4343. [[CrossRef](#)]
12. Pan, G.; Lei, H.; Deng, Y.; Fan, L.; Yang, J.; Chen, Y.; Ding, Z. On Secrecy Performance of MISO SWIPT Systems With TAS and Imperfect CSI. *IEEE Trans. Commun.* **2016**, *64*, 3831–3843. [[CrossRef](#)]
13. Zhang, H.; Du, J.; Cheng, J.; Long, K.; Leung, V.C.M. Incomplete CSI Based Resource Optimization in SWIPT Enabled Heterogeneous Networks: A Non-Cooperative Game Theoretic Approach. *IEEE Trans. Wirel. Commun.* **2018**, *17*, 1882–1892. [[CrossRef](#)]

14. Bi, Y.; Chen, H. Accumulate and Jam: Towards Secure Communication via A Wireless-Powered Full-Duplex Jammer. *IEEE J. Sel. Top. Signal Process.* **2016**, *10*, 1538–1550. [[CrossRef](#)]
15. Liu, H.; Kim, K.J.; Kwak, K.S.; Poor, H.V. QoS-Constrained Relay Control for Full-Duplex Relaying with SWIPT. *IEEE Trans. Wirel. Commun.* **2017**, *16*, 2936–2949. [[CrossRef](#)]
16. Tang, X.; Deng, Y.; Cai, Y.; Yang, W.; Nallanathan, A. Analyzing Power Beacon Assisted Multi-Source Transmission Using Markov Chain. *IEEE Access* **2019**, *7*, 3486–3499. [[CrossRef](#)]
17. Zeng, Y.; Zhang, R. Full-Duplex Wireless-Powered Relay with Self-Energy Recycling. *IEEE Wirel. Commun. Lett.* **2015**, *4*, 201–204. [[CrossRef](#)]
18. Gans, M.J. The Effect of Gaussian Error in Maximal Ratio Combiners. *IEEE Trans. Commun. Technol.* **1971**, *19*, 492–500. [[CrossRef](#)]
19. Suraweera, H.A.; Smith, P.J.; Shafi, M. Capacity Limits and Performance Analysis of Cognitive Radio with Imperfect Channel Knowledge. *IEEE Trans. Veh. Technol.* **2010**, *59*, 1811–1822. [[CrossRef](#)]
20. Huang, Y.; Li, C.; Zhong, C.; Wang, J.; Cheng, Y.; Wu, Q. On the Capacity of Dual-Hop Multiple Antenna AF Relaying Systems with Feedback Delay and CCI. *IEEE Commun. Lett.* **2013**, *17*, 1200–1203. [[CrossRef](#)]
21. Gradshteyn, I.S.; Ryzhik, I.M. *Table of Integrals, Series, and Products*, 7th ed.; Elsevier/Academic Press: Amsterdam, The Netherlands, 2007; p. 1172.
22. Zhou, X.; Guo, J.; Durrani, S.; Renzo, M.D. Power Beacon-Assisted Millimeter Wave Ad Hoc Networks. *IEEE Trans. Commun.* **2018**, *66*, 830–844. [[CrossRef](#)]



© 2019 by the authors. Licensee MDPI, Basel, Switzerland. This article is an open access article distributed under the terms and conditions of the Creative Commons Attribution (CC BY) license (<http://creativecommons.org/licenses/by/4.0/>).